# Growth and characterization of high-density mats of single-walled carbon nanotubes for interconnects

J. Robertson,[1,a)] G. Zhong,[1] H. Telg,[2] C. Thomsen,[2] J. H. Warner,[3] G. A. D. Briggs,[3] U. Dettlaff-Weglikowska,[4] and S. Roth[4]
[1]*Department of Engineering, University of Cambridge, Cambridge CB3 0FA, United Kingdom*
[2]*Institut für Festkörperphysik, Technische Universität Berlin, 10623 Berlin, Germany*
[3]*Department of Materials, University of Oxford, Oxford OX1 3PH, United Kingdom*
[4]*Max Planck Institut für Festkörperphysik, D-70569 Stuttgart, Germany*

(Received 18 September 2008; accepted 23 September 2008; published online 22 October 2008)

We grow high-density, aligned single wall carbon nanotube mats for use as interconnects in integrated circuits by remote plasma chemical vapor deposition from a Fe–$Al_2O_3$ thin film catalyst. We carry out extensive Raman characterization of the resulting mats, and find that this catalyst system gives rise to a broad range of nanotube diameters, with no preferential selectivity of semiconducting tubes, but with at least 1/3 of metallic tubes. © *2008 American Institute of Physics*. [DOI: 10.1063/1.3000061]

Carbon nanotubes have unique properties that make them valuable for electronic applications. Some applications such as transistors require semiconducting nanotubes, while others such as interconnects in integrated circuits (ICs) or conducting membranes require metallic nanotubes. The nanotube type can be selected after growth by density gradient centrifugation and other methods,[1] but for IC applications, economics requires nanotubes grown in place. A number of groups have shown an ability to preferentially grow one type of nanotube,[2–5] however, this is usually semiconducting tubes. It is therefore necessary to demonstrate that preferential growth of metallic tubes is also possible.

The demand to use carbon nanotubes as IC interconnects arises from the continued downscaling of semiconductor device dimensions, which means that the current densities in interconnects will soon exceed the electromigration limit of copper, $\sim 6 \times 10^6$ A cm$^{-2}$. Carbon nanotubes are one of the few possible materials that can carry higher current densities than this.[6,7] This led to intensive research on how to integrate nanotube interconnects into complementary metal-oxide semiconductor (CMOS) technology.[7–10] Nanotubes satisfy three future requirements for interconnects; a high current density, the possibility of ballistic transport, and scalability of size to very small diameters.[7] However, it has been difficult to integrate nanotubes into CMOS technology by growing them in place, while achieving performances comparable to existing Cu interconnects.[10]

Carbon nanotubes are one-dimensional conductors, and so their conductance is limited by one quantum of conductance $G_0$ per conducting channel. This resistance of 12.6 kΩ acts as a series resistance, and so we want as many conducting channels in parallel as possible to minimize the overall resistance. We must therefore produce either a very high density of single-walled nanotubes (SWNTs) of up to $10^{14}$ cm$^{-2}$, or a high density of thin multiwalled nanotubes (MWNTs) with contact made to every wall.

Here we focus on the growth and characterization of high-density mats of metallic SWNTs. The nanotubes are grown by chemical vapor deposition (CVD). Interconnects are back end of line components and so they have an upper process temperature of ~400 °C. Thus, there are five requirements on the CVD; high density, low growth temperature, high fraction of metallic nanotubes, growth on conducting surfaces, and low defect nanotubes.

The highest density of SWNTs grown by catalytic CVD are so far found in vertically aligned nanotube mats. It is interesting that the highest density mats are grown using two particular catalyst systems, Fe on an $Al_2O_3$ support or a Co–Mo catalyst. The Fe–$Al_2O_3$ system was used in the "supergrowth" process of Hata and co-workers[11,12] and also in the remote plasma CVD process of Zhong *et al.*[13,14] Here, we are interested not in the height of the forest or the role of water, only SWNT mat density, and more importantly that both groups use the *same* Fe–$Al_2O_3$ catalyst system. Similarly, it is interesting that the aligned SWNT mats of Maruyama *et al.*[5,15] and Resasco and co-workers[4,16,17] use a similar Co–Mo catalyst.

It was found that lowering the growth temperature for Co–Mo catalysts narrows the chirality distribution,[5,16] with a higher fraction of semiconducting tubes. This is unsuitable for interconnects, so we develop further the Fe–$Al_2O_3$ catalyst system. The conductivity and mat density of such nanotubes have been measured previously.[10,14,18]

The present samples were grown using a remote microwave plasma-assisted CVD method using a 90:10 $H_2$:$CH_4$ mixture as the feed gas at 15 mbar pressure at 650 °C.[13] The catalyst consists of 0.5–1.0 nm Fe sputtered onto 10 nm of Al, with 0.5 nm of Al layer on top. The Al is oxidized to $Al_2O_3$ during transfer to the growth chamber.

The nanotubes grow from the nanostructured catalyst. In order to activate the catalyst, it is converted from a thin film form into a series of nanoparticles on the support, its active chemical state.[18–20] In order to allow a low growth temperature, this requires careful control of the restructuring step, separately before growth. Annealing must be carried out in a reducing or vacuum environment, depending on the catalyst, but prior to the admittance of the growth gas. This then allows growth at temperatures as low as 400 °C for both MWNTs and SWNTs.

We have characterized our SWNTs in detail. The usual means to measure the chirality distribution is by photoluminescence excitation spectroscopy (PLE). However, PLE only

a)Electronic mail: jr@eng.cam.ac.uk.

 

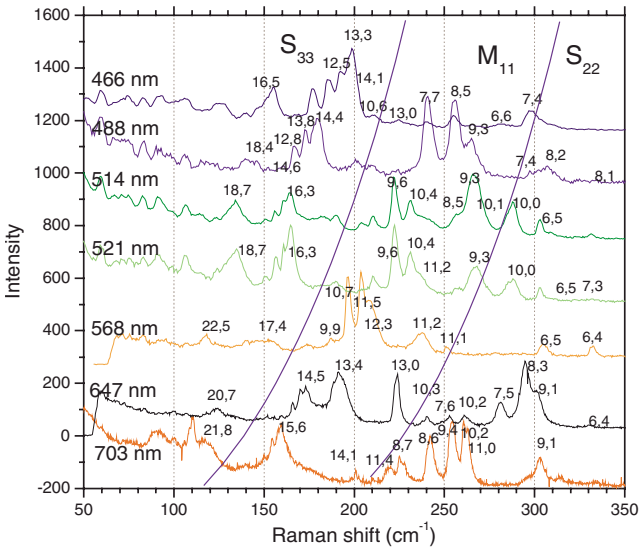


FIG. 1. (Color online) Raman spectra of the radial breathing modes of a SWNT mat sample, excited at the indicated laser wavelengths. The spectra range is divided into zones corresponding to modes of metallic ($M11$) and semiconducting tubes ($S22$,$S33$). Chiral index assignments are shown.

probes semiconducting tubes. We use instead resonant Raman spectroscopy,[21,22] which sees both types. The Raman measurements were carried out on a Dilor XY800 spectrometer with triple monochromator and Ar–Kr laser and tunable lasers. The samples are probed directly without dispersion in surfactants.

Figure 1 shows the radial breathing mode (RBM) part of the Raman spectra of the samples measured at various laser wavelengths. A notable feature of Fig. 1 is that the RBMs cover a wide range of wavenumbers, which is equivalent to a wide range of nanotube diameters, and in addition the peaks are sharp, which helps to assign them to a specific chiral indices, $n,m$.

We have made detailed chiral index assignments of the RBM peaks. First, the RBM frequency is known to vary inversely with the nanotube diameter, $d$. Second, a mode is excited only when the laser energy is resonant with a particular electronic transition between subbands of that nanotube diameter. The transitions between subbands each vary roughly as $1/d$, but with well-defined trends away from this simple dependence. The transitions are displayed on a "Kataura plot" as in Fig. 2(a). The plotted transitions consist of the lower energy $S_{11}$ and $S_{22}$ levels of semiconducting tubes, followed by the $M_{11}$ levels of metallic tubes, followed by the higher order $S_{33}$ and $S_{44}$ bands of semiconducting tubes. The trends away from the simple $1/d$ dependence fall into families, according to whether $\nu=(n\text{-}m, \mathrm{mod}\ 3)=-1,0,$ or $+1$. The nanotube diameter is given by $d=a_0(n^2+nm+m^2)^{1/2}/\pi$, where $a_0=2.461$ Å is the graphite lattice constant.

The Kataura plot of transition energies is based on the third-neighbor tight-binding plot of Popov *et al.*[23] which includes the effects of trigonal warping (Fig. 2). It does not include the exciton binding energy, which can be included empirically by an upward shift of ~0.3 eV for the $S_{11}$, $S_{22}$, and $M_{11}$ transitions. Recently, Araujo *et al.*[24] concluded that the higher order transitions $S_{44}$ and $S_{55}$ have delocalized excitons with much small binding energies, so these gaps are not shifted. The presence of a large range of tube diameters in our sample and the rather sharp spectra allows these

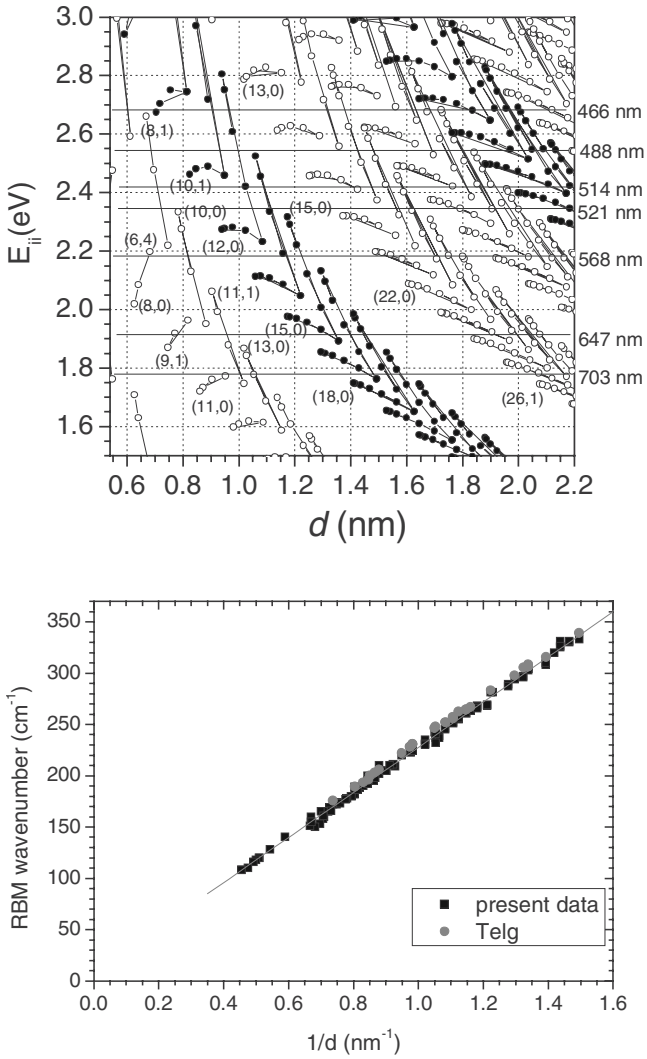


FIG. 2. (a) Subband energy vs diameter plot used for the assignment. (b) Fitting of the RBM wavenumber to the nanotube diameter, Eq. (1), compared to the Telg fit.

higher order $S_{33}$ and $S_{44}$ transitions to be fitted. Some of the assignments are given in Fig. 1.

The RBM frequencies have been fitted with the usual relationship

$$\omega = C_1/d + C_2 \tag{1}$$

to give $C_1=220.4\pm0.7$ and $C_2=7.4\pm0.7$, as in Fig. 3. This compares with $C_1=214.4$ and $C_2=18.7$ found by Telg *et al.*[21] or $C_1=217.8$ and $C_2=15.7$ by Araujo *et al.*[24] for SWNTs dispersed in sodium dodecyl sulfate surfactant. The trend of aligned forests to have lower $C_2$ values follows that found by Araujo *et al.*[25] for supergrowth samples.

The RBM spectra show a number of interesting features. A notable feature is that the fitted RBMs cover a wide range of wavenumbers, equivalent to a wide range of nanotube chiralities and diameters (0.8–2.2 nm). This is consistent with transmission electron microscopy images for our samples in Fig. 3. It is also consistent with Yamada *et al.*,[12] who found a wide range of diameters in their electron microscope study, from SWNTs to double walled nanotubes to MWNT.

The wide range of chiralities in Fig. 1 indicates that both metallic and semiconducting nanotubes are present. The re-

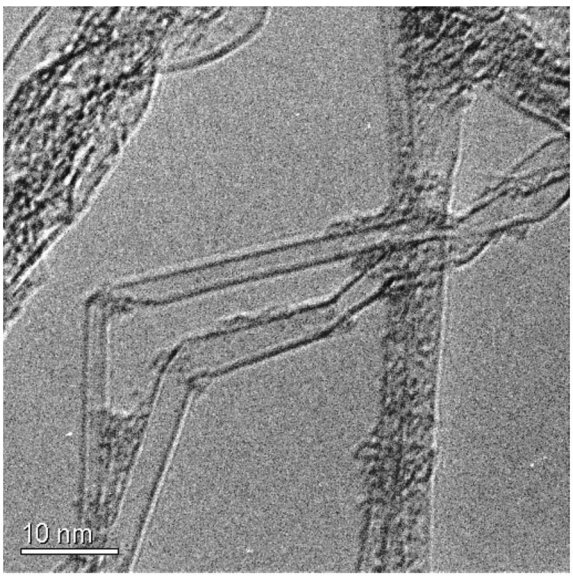


FIG. 3. Transmission electron microscope image of the nanotube sample.

gions of the $S_{22}$ and $S_{33}$ transitions of semiconducting tubes and $M_{11}$ of metallic tubes are shown. Clearly, there is no narrowing of the chirality distribution in our material, and the presence of many metallic tubes is suitable for use as interconnects. We therefore conclude that the $Fe-Al_2O_3$ catalyst is more suitable than Co–Mo catalysts for interconnect applications requiring metallic nanotubes.

We further quantified the abundance distribution by calibrating the Raman matrix elements against spectra for HiPCo samples which are usually assumed to have the random distribution with a metallic to semiconducting ratio of 1:2. We use the empirical dependence of matrix element on chiral angle and diameter in Luo *et al.*[26] as a guide. We find that our samples have a near random mixture of metallic and semiconducting chiralities. This means that our nanotubes are suitable for use as interconnects; there has been no preference for semiconducting tubes.

This is significant because recently Qu *et al.*[3] claimed a 96% preferential growth of semiconducting tubes using a rather similar catalyst system. On the other hand, we have found that it is not just a Fe catalyst that controls nanotube type, it can be varied by using different Fe precursors. This indicates that the restructuring process controls what type of nanotubes likely to grow. Generally, control of nanotube character during growth still needs further effort.

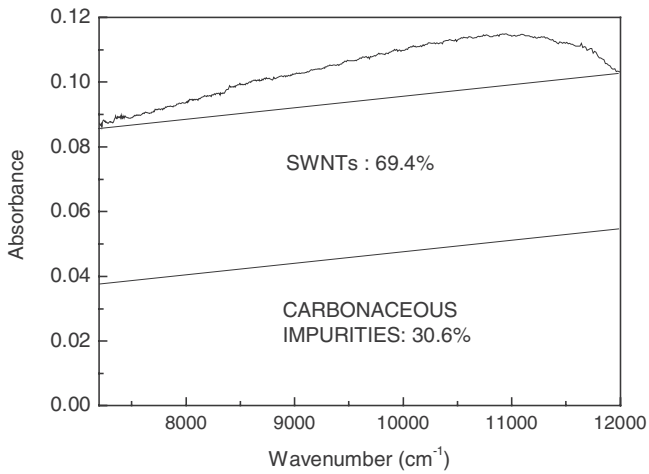


FIG. 4. Infrared spectra of $S_{22}$ subband and background for purity analysis.

Infrared absorption is often used to determine sample purity,[27] which works best for a rather narrow diameter distribution. However, the standard calibrations of assigning a background to graphitic carbon must be readjusted when there is a much wider diameter distribution, as here. From Fig. 4, we derive a purity of 70%.

In summary we have shown that high-density SWNT mats grown from specific catalyst systems can have an adequate fraction of metallic nanotubes. The catalyst system will now be developed for a metallic support.

The authors thank the financial support of EC projects Canape and Viacarbon, and J.R. thanks the A von Humboldt Foundation for a research award for his stay at TU Berlin.

[1]M. C. Hersam, Nat. Nanotechnol. **1**, 60 (2006); **3**, 387 (2008).
[2]Y. Li, D. Mann, M. Rolandi, W. Kim, A. Ural, S. Huang, A. Javey, D. Wang, E. Yenilmez, Q. Wang, J. F. Gibbons, Y. Nishi, and H. Dai, Nano Lett. **4**, 317 (2004).
[3]L. Qu, F. Du, and L. Dai, Nano Lett. **8**, 2682 (2008).
[4]S. M. Bachilo, L. Balzano, J. E. Herrera, F. Pompeo, D. E. Resasco, and R. B. Weisman, J. Am. Chem. Soc. **125**, 11186 (2003).
[5]Y. Miyauchi, S. Chiashi, Y. Murakami, Y. Hayashida, S. Maruyama, Chem. Phys. Lett. **387**, 198 (2004).
[6]J. Y. Park, S. Rosenblatt, Y. Yaish, V. Sazonova, H. Ustunel, S. Braig, T. A. Arias, P. W. Bronner, and P. L. McEuen, Nano Lett. **4**, 517 (2004).
[7]B. Q. Wei, R. Vajtai, and P. M. Ajayan, Appl. Phys. Lett. **79**, 1172 (2001).
[8]F. Kreupl, A. P. Graham, M. Liebau, G. S. Duesberg, R. Seidel, and E. Unger, Tech. Dig. - Int. Electron Devices Meet. **2004**, 683.
[9]M. Nihei, A. Kawabata, D. Kondo, and Y. Awano, Jpn. J. Appl. Phys., Part 1 **43**, 1856 (2004); **44**, 1626 (2004).
[10]D. Yokoyama, T. Iwasaki, K. Ishimaru, S. Sato, T. Hyakushima, M. Nihei, Y. Awano, and H. Kawarada, Jpn. J. Appl. Phys., Part 1 **47**, 1985 (2008).
[11]K. Hata, D. N. Futuba, K. Mizuno, T. Namai, M. Yumura, and S. Ijima, Science **306**, 1362 (2004).
[12]T. Yamada, T. Namai, K. Hata, D. N. Futaba, K. Mizuno, J. Fan, M. Yudasaka, M. Yumura, and S. Iijima, Nat. Nanotechnol. **1**, 131 (2007).
[13]G. Zhong, T. Iwasaki, K. Honda, Y. Ohdomari, and H. Kawarada, Jpn. J. Appl. Phys., Part 1 **44**, 1558 (2004).
[14]G. Zhong, T. Iwasaki, and H. Kawarada, Carbon **44**, 2009 (2006).
[15]M. Hu, Y. Murakami, M. Ogura, S. Maruyama, and T. Okubo, J. Catal. **225**, 230 (2004).
[16]L. Zhang, Y. Q. Tan, and D. E. Resasco, Chem. Phys. Lett. **422**, 198 (2006).
[17]J. E. Herrera, L. Balzano, A. Brogna, and D. E. Resasco, J. Catal. **204**, 129 (2001).
[18]C. Mattevi, C. T. Wirth, S. Hofmann, R. Blume, M. Cantoro, C. Ducati, C. Cepek, A. Knop-Gericke, A. Goldoni, R. Schlogl, and J. Robertson, J. Phys. Chem. C **112**, 12207 (2008).
[19]M. Cantoro, S. Hofmann, S. Pisana, V. Scardaci, A. Parvez, C. Ducati, A. C. Ferrari, A. M. Blackburn, K. Y. Wang, and J. Robertson, Nano Lett. **6**, 1107 (2006).
[20]S. Hofmann, R. Sharma, C. Ducati, G. Du, C. Mattevi, C. Cepek, M. Cantoro, S. Pisana, A. Parvez, F. Cervantes-Sodi, A. C. Ferrari, R. E. Dunin-Borkowski, and J. Robertson, Nano Lett. **7**, 602 (2007).
[21]H. Telg, J. Maultzsch, S. Reich, F. Heinrich, and C. Thomsen, Phys. Rev. Lett. **93**, 177401 (2004); J. Maultzsch, H. Telg, S. Reich, and C. Thomsen, Phys. Rev. B **72**, 205438 (2005).
[22]C. Fantini, A. Jorio, M. Souza, M. S. Strano, M. S. Dresselhaus, and M. A. Pimenta, Phys. Rev. Lett. **93**, 147406 (2004).
[23]V. N. Popov and L. Henard, Phys. Rev. B **70**, 115407 (2004).
[24]P. T. Araujo, S. K. Doorn, S. Kilina, S. Tretiak, E. Einarsson, and A. Jorio, Phys. Rev. Lett. **98**, 067401 (2007).
[25]P. T. Araujo, I. O. Maciel, P. B. C. Pesce, M. A. Pimento, S. K. Doorn, and A. Jorio, Phys. Rev. B **77**, 241403 (2008).
[26]Z. Luo, F. Papadimmitrakopoulos, and S. K. Doorn, Appl. Phys. Lett. **88**, 073110 (2006).
[27]M. E. Itkis, D. E. Perea, and R. C. Haddon, Nano Lett. **3**, 309 (2003).